

## PVP2009-77370

### EFFECT OF FREQUENCY AND SHAPE OF THERMAL CYCLING ON THE DAMAGE OF MULTI-MATERIAL UNDER THERMO-ELASTO-PLASTIC BEHAVIOUR

**Bilal Taher**  
SET Laboratory, University of  
Technology of Belfort – Montbéliard,  
Belfort, France  
bilal.taher@utbm.fr

**Said Abboudi**  
SET Laboratory, University of  
Technology, Belfort – Montbéliard,  
Belfort, France  
said.abboudi@utbm.fr

**Rafic Youness**  
3M laboratory, Faculty of  
Engineering, Lebanese University,  
Beirut, Lebanon  
ryounes@ul.edu.lb

#### ABSTRACT

In this study, we propose a numerical analysis of the thermo-elasto-plastic behavior of a multi-material and its damage under thermal cyclic solicitations. The study is done in two dimensions on a cylindrical multi-material subjected to a periodic heat flux on the internal face and to a convective heat transfer condition on the opposite external face. Lateral faces are supposed to be isolated. The sample is supposed to be fixed in the axial direction and free in the other. The damage model is based on the works of Lemaître and Chaboche.

Numerical results are presented for different shapes of heat flux cycling (triangular, square and sinusoidal excitations, function of time and space) and for a range of periods. We do a comparison of the multi-material damage under these different thermal excitations.

The study is concluded by some advice on the use and avoidance of some values of periods, and shapes for the thermal load excitation, in order to obtain the maximum lifetime of the multi-material under thermo-elasto-plastic behavior.

#### INTRODUCTION

The study of metallic components solicited with high temperatures has really started in fifties by the aeronautic industry and with the beginning of the nuclear industry. These materials have been submitted to very high temperatures, sometimes more than half the temperature of fusion. In this

range of temperatures, their mechanical properties are considerably modified and / or the damage mechanisms are multiplied. The solicitations cycles, to which these metallic structures are submitted, frequently cause cyclic inelastic deformations. Every system or mechanical component is likely to be subject to a thermo-elasto-plastic coupling. This is due to the fact that the abrupt variation and the periodicity of the temperature influence the fatigue of constituent materials. This consequently leads to the complete destruction of the materials.

The presence of thermal and mechanical loads in every system motivates the researchers to work in this domain and especially in the field of variable load and its influence, by means of period solicitation, amplitude and shape, on the material damage [1-5].

Almost, all previous works address only the effect of mechanical load on the damage. We can find experimental studies as well as studies done by means of simulation and modeling [3], [6], [8-9].

The others of [1-2] conducted a study by the use of very high frequency mechanical vibration. They concluded that there is a relationship between the load frequency and the fatigue of the material under mechanical solicitation. They proved also that there is a fatigue variation relative to the material resonance value. Based on the above studies, it is very important to study the influence of the frequency variation on the lifetime and on the number of cycles to damage.

This does not mean that the thermo-mechanical effect was not studied before. There are some advanced studies that analyze the thermo-mechanical damage under thermal load, but their studies are still limited by the assumption that the thermal load is constant [10-11]. The mechanical load is considered as variable. This assumption is taken in order to simplify the study by neglecting the transient regime of the thermal load. In general, these approaches underestimate the thermo-elasto-plastic behavior of these materials and as a result their behavior in fatigue [12].

Some other studies take into consideration the transient regime of a variable thermal load, but these are experimental studies only and are not done by means of physical models [14]. In fact, there is an important difficulty in the finding of the correct damage model, because there is no damage law that takes into consideration a variable thermal load. This is verified by the presence of a lot of mechanical damage laws in the literature, but of only one law for isothermal damage [6]. At the level of our knowledge, there is not a variable thermal damage law that can be used in thermo-mechanical damage modeling.

From another point of view, the experimental works that study the effect of variable thermal load on the damage, and in order to show the effect of the frequency of this thermal load, consider only a limited number of values for the frequency, and can not extend their studies to all frequency ranges because this will be more and more expensive to experiment with. [10], [14].

Also, in the literature, there are no thermo-mechanical damage studies on multi-materials. In fact, for the damage study, the existing laws of damage, in the scientific field, especially those by [6-7] cannot be applied on multi-materials; they can only be applied on simple and unique materials.

Furthermore, the studies of both layers, supposed to be in perfect contact, lead to perfect theoretical results; for example, they lead to an ideal heat transfer and the stress is distributed regularly and is discontinuous at the level of the interface between layers.

It is also evident that in a two-layer material, there is a mutual influence of one material on the other; we cannot have an abrupt variation of the thermal and mechanical properties at the level of the joint. At this level, we have a certain region in which the values of thermal and mechanical properties are supposed to vary between those of the constituting materials. This reasoning imposes the necessity of searching for a method of correction based on the principle of homogenization of multi-materials in a single equivalent material. This latter has to undergo the study of the damage under thermo-mechanical stress [15-16].

The homogenization approach proposed in [13] replaces the multi-material with a unique material having constant and equivalent thermo-physical properties obtained by means of models that allow us to have similar temperatures in both materials and in equivalent materials as well.

This approach cannot be used to obtain the correct value of the damage in each point of the material because in reality the temperature cannot be constant and similar in all points. For this reason, we use herein the homogenization approach detailed in [16] which replaces the two materials with a unique one where a polynomial interpolation of the properties is

used. This technique is validated in this work and gives good results.

After this introduction a set of abbreviations and symbols used in this paper are given. A description of the sample studied is detailed in section I. The mathematical formulation of the thermal and the thermo-mechanical problems and damage is shown in section II. In section III, we carry out a numerical analysis of the problem. Our conclusion and perspectives are given in section IV.

## NOMENCLATURE

### Symbols:

$B_0$	constant of the damage law $MPa$
$C$	calorific capacity, $J/Kg.K$
$D$	number of cycles to damage
$E$	Elasticity modulus, $Pa$
$e_i$	thickness of the layer $i = 1, 2$
$e$	thickness of the body $e = e_1 + e_2$
$h$	coefficient of convection, $W/m^2.K$
$K_y$	coefficient of plastic resistivity $MPa$
$L$	length $m$
$LFT$	lifetime $S$
$M_y$	exponent of work hardening
$Q$	heat flux density, $W/m^2$
$r$	radial coordinate, $m$
$R$	volume heat source $W/m^3$
$T$	temperature, $K$
$T_0$	initial temperature, $K$
$T_a$	ambient temperature, $K$
$U$	displacement according to $r$ , $m$
$V$	displacement according to $z$ , $m$
$z$	axial coordinate, $m$

### Greek letters:

$\alpha$	expansion coefficient, $m/K$
$\beta$	exponent of the damage law
$\rho$	density, $Kg/m^3$
$\lambda$	thermal conductivity, $W/m.K$
$\nu$	Poisson coefficient
$\sigma$	stress tensor, $Pa$
$\bar{\sigma}$	average stress tensor, $Pa$
$\sigma_l$	limit stress tensor, $Pa$
$\sigma_M$	maximum stress tensor, $Pa$
$\sigma_s$	applied stress, $Pa$
$\sigma_u$	ultimate stress tensor, $Pa$
$\sigma_y$	elastic limit stress, $Pa$
$\epsilon$	deformation tensor
$\epsilon^e$	elastic deformation tensor
$\epsilon^p$	plastic deformation tensor
$\epsilon^{th}$	thermal deformation tensor
$\epsilon^c$	creep deformation tensor
$\tau$	period, $s$

## I- PRESENTATION OF THE PROBLEM

The body studied is constituted of two layers of different materials, the sub-base "Material-1" is a layer made of stainless steel and the other "Material-2" is made of Steel Fig. 1. The physical specifications of these two materials are presented in Table 1.

The internal surface of the sample is submitted to a periodic heat flux and the external surface is submitted to a convective heat transfer condition with the ambient. The left and right sides are supposed to be insulated.

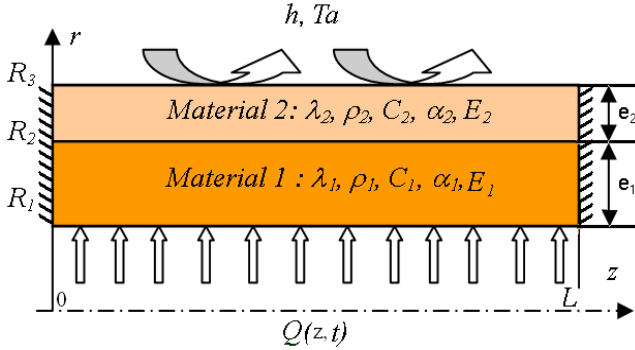


Figure 1: The studied sample

The equivalent material of the system described above is obtained by using a polynomial interpolation of the physical parameters  $\phi = (\rho, c, \lambda, \alpha, E(T))$ , Fig. 2:

$$\phi(r) = \sum_{k=0}^n a_k r^k \quad (1)$$

	Stainless steel	Steel
$\rho$ : density	7854 kg/m <sup>3</sup>	7854 kg/m <sup>3</sup>
$c$ : heat capacity	477 J/Kg.°K	434 J/Kg.°K
$\lambda$ : thermal conductivity	35 W/m°K	60.5 W/m°K
$\alpha$ : expansion coefficient	15.10 <sup>-6</sup> m/K	11.8.10 <sup>-6</sup> m/K
$\nu$ : poisson coefficient	0.3	0.3
$L$ : length	0.6 m	0.6 m
$R_1$ : internal radius	0.1 m	0.1 m
$e$ : thickness	$e_1 = 0.03$ m	$e_2 = 0.03$ m

Table 1: Physical specifications of materials [17]

Note here that this study is applicable to any material having variable physical parameters. So, it is not important here to identify the material presented in Fig. 2 and to specify the materials from which it is generated. The essential thing to keep in mind is that we have a material having variable physical parameters according to  $r$ .

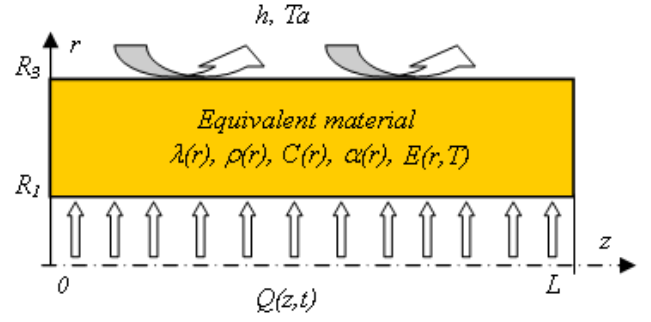


Figure 2: Equivalent Material

## II- MATHEMATICAL FORMULATION

Our approach consists of considering the thermal equation while taking into account the presence of heat created by the elasto-plastic behavior of the material and caused by the external thermal solicitation. This thermal equation helps us to observe the evolution of the distribution of the temperature and then the thermal behavior of the body with respect to the thermal excitation applied to it. Then the thermo-elasto-plastic problem is considered to observe the evolution of the distributions of the deformations of the body and then the thermo-mechanical behavior of the material.

In the following paragraph, the mathematical formulations are presented respectively for both the multi-material and the equivalent material. The contact between the two layers is considered to be perfect.

### II.1 Thermal Formulation

In the thermo-mechanical coupling system, the transient heat transfer balance equation [6] and [18-20] is:

$$\rho C \dot{T} = \text{div}(\lambda \vec{\text{grad}} T) + \sigma : \dot{\epsilon}^p - A_k \dot{V}_k + R + T \left[ \frac{\partial \sigma}{\partial T} : \dot{\epsilon}^e + \frac{\partial A_k}{\partial T} \dot{V}_k \right] \quad (2)$$

Where:

$\text{div}(\lambda \vec{\text{grad}} T)$  is the adiabatic evolution

$A_k \dot{V}_k$  is the non-recoverable energy stored in the material.

$\sigma : \dot{\epsilon}^p$  is the plastic energy

$T \frac{\partial \sigma}{\partial T} : \dot{\epsilon}^e$  is the energy of thermo-mechanical coupling

$T \frac{\partial A_k}{\partial T} \dot{V}_k$  is the variation of the non-recoverable energy

stored in the material with the temperature.

And finally  $R$  is the internal heat production created by external sources.

In this work, the following hypotheses are supposed:

- The internal heat generation is neglected  $R = 0$ .
- The energy belongs to the residual micro-stress field accompanying the increase of the dislocation density [6] represents only 5 to 10 % of the value of  $\sigma : \dot{\epsilon}^p$ . Then this energy is neglected,

$$A_k \dot{V}_k \cong 0 \text{ and } T \frac{\partial A_k}{\partial T} \dot{V}_k \cong 0 \quad (3)$$

**II.1.1 Theoretical materials:** Under these hypotheses, the theoretical thermal model of the studied system is:

$$(\rho C)_i \cdot \frac{\partial T_i}{\partial t} = \lambda_i \left( \frac{1}{r} \frac{\partial}{\partial r} \left( r \frac{\partial T_i}{\partial r} \right) + \frac{\partial^2 T_i}{\partial z^2} \right), i=1, 2, \quad (4)$$

$$+ T_i \frac{\partial \sigma_i}{\partial T} : \frac{\partial \varepsilon_i^e}{\partial t} + \sigma_i : \frac{\partial \varepsilon_i^p}{\partial t}$$

With:  $i=1$  (stainless steel),  $i=2$  (Steel)

Submitted to the following initial and boundary conditions:

$$T(r, z, 0) = T_0 \quad \text{at } t=0 \quad (5)$$

$$-\lambda_1 \frac{\partial T}{\partial r} = \phi(z, t) \quad r = R_1 \quad 0 < z < L \quad (6)$$

$$-\lambda_2 \frac{\partial T}{\partial r} = h(T - T_f) \quad r = R_3 \quad (7)$$

$$-\lambda_i \frac{\partial T}{\partial z} \Big|_{z=0} = -\lambda_i \frac{\partial T}{\partial z} \Big|_{z=L} = 0, \quad i=1, 2 \quad (8)$$

At the interface, the continuity of the heat flux and the temperatures is respected (perfect contact):

$$T_1 = T_2, \quad r = R_2 \quad (9)$$

$$-\lambda_1 \frac{\partial T}{\partial r} = -\lambda_2 \frac{\partial T}{\partial r}, \quad r = R_2 \quad (10)$$

**II.1.2 Homogeneous material:** For the homogeneous material, the thermal equation is as follows:

$$(\rho C)(r) \frac{\partial T}{\partial t} = \left( \frac{1}{r} \frac{\partial}{\partial r} \left( r \lambda(r) \frac{\partial T}{\partial r} \right) + \lambda(r) \frac{\partial^2 T}{\partial z^2} \right). \quad (11)$$

$$+ T \frac{\partial \sigma}{\partial T} : \frac{\partial \varepsilon^e}{\partial t} + \sigma : \frac{\partial \varepsilon^p}{\partial t}$$

Where  $T$ ,  $\sigma$ ,  $\varepsilon^e$  and  $\varepsilon^p$  are functions of  $(r, z, t)$ .

With the following initial and boundary conditions:

$$T(r, z, 0) = T_0 \quad t=0 \quad (12)$$

$$-\lambda(r) \frac{\partial T}{\partial r} = \phi(z, t) \quad r = R_1 \quad (13)$$

$$-\lambda(r) \frac{\partial T}{\partial r} = h(T - T_0) \quad r = R_3 \quad (14)$$

$$-\lambda(r) \frac{\partial T}{\partial z} \Big|_{z=0} = -\lambda(r) \frac{\partial T}{\partial z} \Big|_{z=L} = 0, \quad R_1 < r < R_3 \quad (15)$$

## II.2 Thermo-mechanical equation in elastic regime

The thermo-mechanical equation in the elastic regime is obtained by the introduction of the thermal deformation in the Lamé mechanical behavior equation [19].

$$\sigma(r, z, t)_{ij} = E(T)_{ij} (\varepsilon_{ij} - \alpha_{ij} (T(r, z, t) - T_0)) \quad (16)$$

**Hypotheses:** The stress is supposed to be unidirectional: the body is fixed in the  $z$  direction and we have  $L/R = 6 \ll 45$ . So, we have no flexion and the maximum of the stress is applied in the fixed (isolated) sides  $z=0$  and  $z=L$ .

The variation of the Young modulus  $E$  is presented in Table 2.

Temperature ( $^{\circ}C$ )	0	05	30	50
Stainless steel (MPa)	96	83	65	46
Steel (MPa)	10	98	80	55

Table 2: Young module  $E$  variation with the temperature [22]

**II.2.1 Theoretical material:** In a matrix form, for axis-symmetric isotropic material,  $\alpha_{rr} = \alpha_{zz} = \alpha$  and  $\alpha_{rz} = 0$

$$\begin{bmatrix} \sigma_{rr} \\ \sigma_{zz} \\ \sigma_{rz} \end{bmatrix}_i = \left( \frac{E}{(1+\nu)(1-2\nu)} \right)_i \begin{bmatrix} 1-\nu & \nu & 0 \\ \nu & 1-\nu & 0 \\ 0 & 0 & \frac{1-2\nu}{2} \end{bmatrix}_i \times \begin{bmatrix} \varepsilon_{rr}^e - \alpha(T-T_0) \\ \varepsilon_{zz}^e - \alpha(T-T_0) \\ \varepsilon_{rz}^e \end{bmatrix}_i \quad (17)$$

Where  $i=1,2$

**II.1.2 Homogeneous material:** For the homogenous material, we can use eq. 17 as the thermo-elastic behavior equation but without the subscript  $i$  and where  $\nu$ ,  $\alpha$  are functions of  $r$ , and  $E$  is function of  $r$  and  $T$ .

## II.3 Plastic formulation

In the plasticity regime, the deformation of the material is formulated by the Ramberg-Osgood equation [6]:

$$\varepsilon^p = \left\langle \frac{\sigma_s - \sigma_y}{K_y} \right\rangle^{M_y} \quad (18)$$

Where  $\sigma_s$  is the applied stress,  $\sigma_y$  is the elasticity limit stress,  $K_y$  is the plastic resistance coefficient,  $M_y$  is the hardening exponent. These parameters are defined in Table 3.

**Hypotheses:** The body is fixed in the  $z$  direction:  $\varepsilon_{zz}^p = 0$ .

The applied stress  $\sigma_s$  is equal to  $\sigma_{zz}$  in our case.

Material	$\sigma_y$ (MPa)	$M_y$	$K_y$ (MPa)
Stainless steel 316 L	133	4.5	435
Steel 35 NCD 16	1200	3.1	3340

Table 3: Plasticity characteristics [6]

**II.3.1 Theoretical materials:** The plastic deformations of the double-layer material are written, considering that:

- Each layer is separated from the other one

- The intermediate deformations are equal,  $\varepsilon_{rr1}^p = \varepsilon_{rr2}^p$ ,

$\varepsilon_{zz1}^p = \varepsilon_{zz2}^p$ , and the decomposition of the two-dimensional plastic deformation, according to the isotropic criteria, is written as follows:

$$\begin{bmatrix} \varepsilon_{rr} \\ \varepsilon_{zz} \end{bmatrix}_i^p = \left[ \left( \frac{\sigma_{zz} - \sigma_y}{K_y} \right)^{M_y} \right]_i, \quad i=1, 2 \quad (19)$$

The parameters  $\sigma_{yi}$ ,  $K_{yi}$ ,  $M_{yi}$ , depend on the nature of the material,  $i = 1$  (stainless Steel),  $i = 2$  (Steel).

**II.3.2 Homogeneous material:** Using the homogeneous principle, the plastic deformation, in this case, can be written by the same expression, eq. 18, where the parameters  $\sigma_y$ ,  $K_y$ ,  $M_y$  are interpolated as a function of  $r$ .

#### II.4 Thermo-elasto-plastic formulation

When the material runs over the elastic region, we can say that this material is in the inelastic phase, so the stress applied to the model is [17]:

$$\sigma_{ii} = \frac{E_{ii}}{(1+\nu_{ii})(1-2\nu_{ii})} \left[ (1-\nu_{ii})\varepsilon_{ii} + \nu_{ii}(\varepsilon_{jj} + \varepsilon_{kk}) \right] - \frac{E_{ii}}{1-2\nu_{ii}} \varepsilon_{ii}^{th} - \frac{E_{ii}}{1+\nu_{ii}} (\varepsilon_{ii}^p + \varepsilon_{ii}^c) \quad (20)$$

Where  $i$  represents  $r, \theta$  or  $z$ .

$\varepsilon_{ii} = \varepsilon_{ii}^e + \varepsilon_{ii}^p + \varepsilon_{ii}^c + \varepsilon_{ii}^{th}$ : is the global deformation.

$\varepsilon_{ii}^e$  is the elastic deformation.

$\varepsilon_{ii}^p$  is the plastic deformation.

$\varepsilon_{ii}^c$  is the creep deformation

$\varepsilon_{ii}^{th} = \alpha_{ii} \Delta T(r, z, t)$  is the thermal deformation.

Taking into account the previsions hypotheses, we can conclude that:  $\varepsilon_{ii}^c = 0$

The study is two-dimensional, so,

$$\varepsilon_{\theta\theta} = \varepsilon_{\theta\theta}^e = \varepsilon_{\theta\theta}^p = \varepsilon_{\theta\theta}^{th} = 0.$$

The two sides of the body are fixed in the  $z$  direction, so,

$$\varepsilon_{zz} = \varepsilon_{zz}^e = \varepsilon_{zz}^p = \varepsilon_{zz}^{th} = 0.$$

The radial deformation is:  $\varepsilon_{rr} = \varepsilon_{rr}^e + \varepsilon_{rr}^p + \varepsilon_{rr}^{th}$ .

**II.4.1 Theoretical materials:** In matrix form and for an axis-symmetric isotropic material, we have:

$$\begin{bmatrix} \sigma_{rr} \\ \sigma_{zz} \end{bmatrix}_i = \left( \frac{E}{(1+\nu)(1-2\nu)} \right)_i \begin{bmatrix} 1-\nu & \nu \\ \nu & 1-\nu \end{bmatrix}_i \begin{bmatrix} \varepsilon_{rr} \\ 0 \end{bmatrix}_i, i=1, 2 \quad (21)$$

$$- \left( \frac{E}{1-2\nu} \right)_i \begin{bmatrix} \alpha_{rr}(T-T_l) \\ \alpha_{zz}(T-T_l) \end{bmatrix}_i - \left( \frac{E}{1+\nu} \right)_i \begin{bmatrix} \varepsilon_{rr}^p \\ 0 \end{bmatrix}_i$$

Where  $\sigma$ ,  $\varepsilon$ ,  $T$  are functions of  $(r, z, t)$ .

**II.4.2 Homogeneous material:** For the homogenous material, we can use eq. 21 as the thermo-elasto-plastic behavior equation but without the subscript  $i$  and where  $\nu, \alpha$  are functions of  $r$ , and  $E$  is function of  $(r, T)$ .

#### II.5 Damage model

The Woehler-Miner law [6] is adopted in this study. The field of validity of this law is mainly the fatigue of the material under periodic solicitations. Woehler-Miner curves represent the relation existing between the number of cycles to

the rupture, the maximum value of the stress  $\sigma_M$  and its average value  $\bar{\sigma}$ .

This law is convenient in our case study. In fact, the mechanical load obtained from the applied thermal solicitations is periodical and the stress applied is only function of  $r$ . Hence, the general formula for this law is:

$$\frac{\delta D}{\delta N} = \frac{\sigma_M - \sigma_l(\bar{\sigma})}{\sigma_u - \sigma_M} \left( \frac{\sigma_M - \bar{\sigma}}{B(\bar{\sigma})} \right)^\beta \quad (22)$$

Where:

$$\sigma_l(\bar{\sigma}) = \bar{\sigma} + \sigma_{l0} \left( 1 - \frac{\bar{\sigma}}{\sigma_u} \right) \quad (23)$$

$$B(\bar{\sigma}) = B_0 \left( 1 - \frac{\bar{\sigma}}{\sigma_u} \right) \quad (24)$$

Where  $\sigma_u$ ,  $\sigma_l$ ,  $B_0$ ,  $\beta$  are defined in Table 4 for the two materials:

Material	$\sigma_u$ MPa	$\sigma_l$ MPa	$B_0$ MPa	$\beta$
Stainless steel	200	650	1144	5.5
Steel	360	2005	6320	3.3

Table4: Coefficients of the damage law [6]

**II.5.1 Theoretical materials:** This damage law is applied to single material. So, theoretically the damage law takes the following model in the multi-material:

$$\frac{\delta D}{\delta N} = \frac{\sigma_M - \sigma_l(\bar{\sigma})_i}{\sigma_{u_i} - \sigma_M} \left( \frac{\sigma_M - \bar{\sigma}}{B(\bar{\sigma})_i} \right)^{\beta_i}, i=1, 2 \quad (25)$$

Where the parameters are predefined

**II.5.2 Homogeneous material:** to calculate the damage in the homogenous material, we can take the same eq. 22. With the parameters  $\sigma_u$ ,  $\sigma_l$ ,  $B_0$ ,  $\beta$  are function of  $r$  as detailed in the homogenous approach described in [16].

### III- NUMERICAL ANALYSIS

#### III.1 Organization of numerical computations

The heat balance equations systems described above for the theoretical and the homogenous materials are solved by the implicit finite difference method. At each time (or iteration), the resulting algebraic system (bloc tridiagonal) is solved by using Thomas algorithm adapted to the bloc tridiagonal matrix. The distribution of the temperature is computed each time and used in the mechanical problem to compute the distribution of the stress and the deformation in the body in elastic regime, elasto-plastic regime and then the damage following the organization chart:

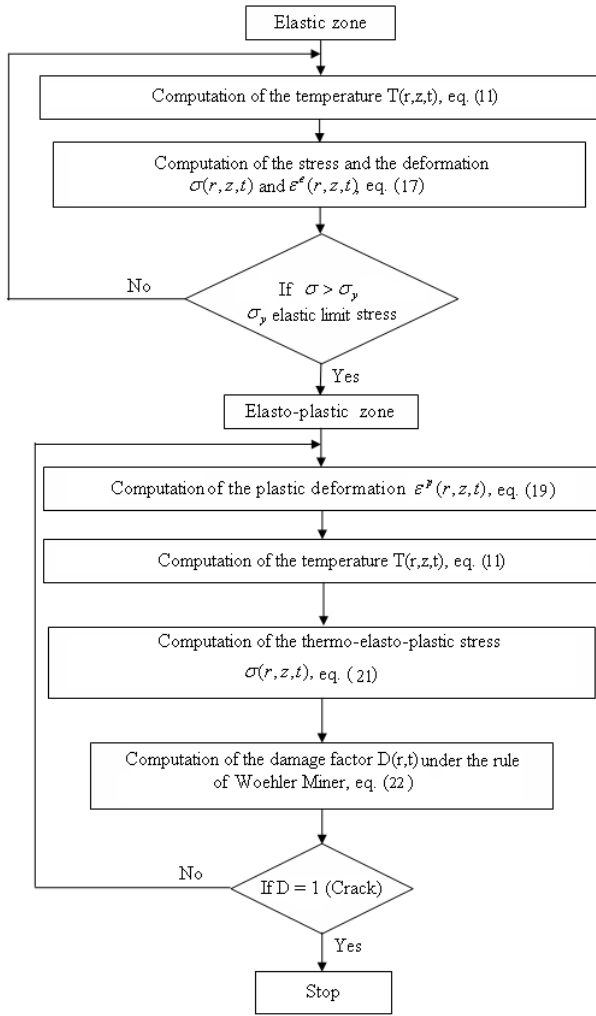


Figure 3: Organizational chart

The numerical study is conducted in the conditions cited in tables 1, 2, 3 and 4 and the following boundary conditions:  
For the thermal problem, we suppose:

$$T_0 = 300 \text{ K}, T_a = 300 \text{ K}, h = 100 \text{ W}/(m^2 \cdot K)$$

The heat fluxes studied are presented in Fig. 4, for the following three cases which represent different industrial applications (for example turbine reactor and cylindrical engine):

Sinusoidal heat flux:

$$Q(z,t) = f(z) \left( 1 + \sin\left(\frac{2\pi}{\tau} t\right) \right) \quad (26)$$

Triangular heat flux:

$$Q(z,t) = \begin{cases} 4f(z) \left( \frac{t}{\tau} - k \right) & 0 \leq \frac{t}{k\tau} < \frac{1}{2} \\ 4f(z) \left( 1 + k - \frac{t}{\tau} \right) & \frac{1}{2} \leq \frac{t}{k\tau} < 1 \end{cases} \quad (27)$$

Square heat flux:

$$Q(z,t) = \begin{cases} 2f(z) & 0 \leq \frac{t}{k\tau} < \frac{1}{2} \\ 0 & \frac{1}{2} \leq \frac{t}{k\tau} < 1 \end{cases} \quad (28)$$

Where:  $f(z) = \frac{4Q_0 z(L-z)}{L^2}$ ,  $Q_0 = 12000 \text{ W}/m^2$ ,

$\tau = 60 \text{ s}$  (period),  $k = 1, 2, \dots, n$  (number of achieved periods)

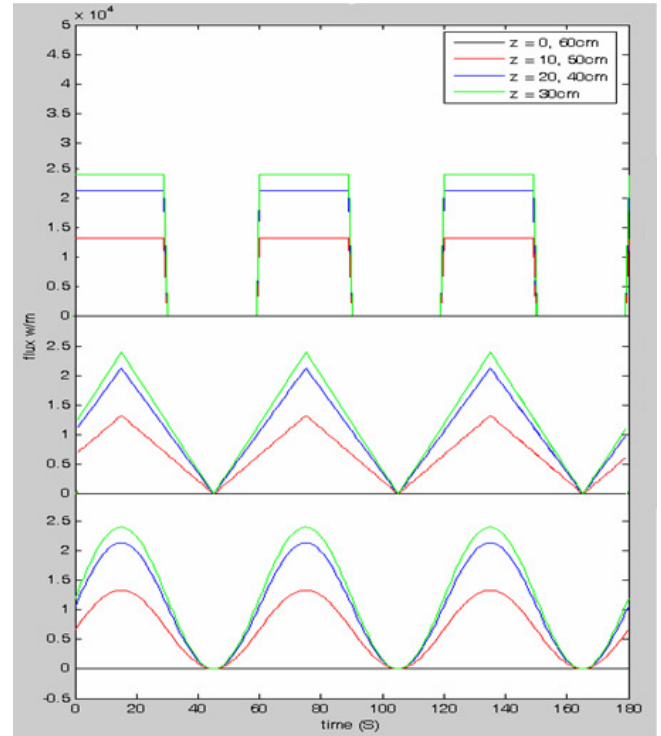


Figure 4: Variation of the applied heat flux (sinusoidal, triangular and square).

For the mechanical problem:

$$V = 0 \text{ at } z = 0 \text{ and } z = L$$

$$U = V = \sigma_{rr} = \sigma_{zz} = \sigma_{rz} = 0 \text{ at } t = 0$$

In these conditions, the distribution of the temperature, for the sinusoidal case, is presented in Fig. 5 at time  $t = 9000 \text{ s}$ .

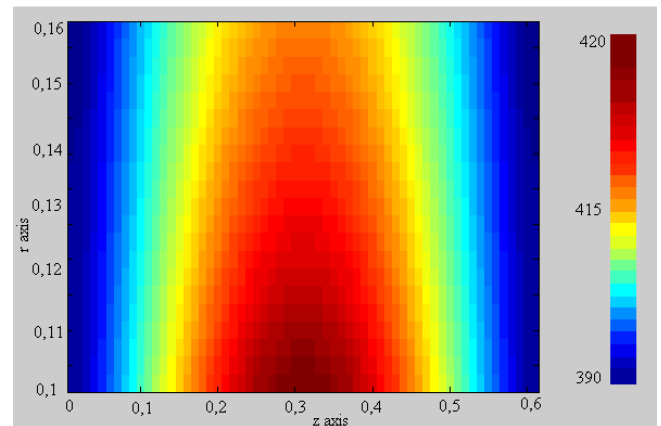


Figure 5: Distribution of the temperature at time 9000 s.

This distribution clearly depends on the variation of the heat flux as well as on the thermal sources resulting from the plastic and elastic deformation. The maximum of the temperature corresponds to the maximum of the heat flux.

### III.2 Numerical results and discussion

In this study, we take into consideration the plastic regime in addition to the elastic regime. In fact, the thermal heat balance formulation takes into account the effect of the plastic and elastic deformations in the thermal sources, see eq. 11. This effect was not studied previously in [15]. In this last work, we did a comparison between the limits of damage by considering various percentages of thickness of these two materials, but this work did not cover the study of the influence of the thermal load (period and shape of the heat flux) with the thickness on the damage.

**A- Influence of the heat flux shape:** The evolutions of the temperature, at three positions ( $r=R_1, R_2$  and  $R_3$ ), are presented on figures 6 for different forms of the heat flux (at  $\tau=60$  s and for  $e_1=e_2=0.03$  m). We can see clearly that the temperature do not follow exactly the shape of the heat flux applied especially for the triangular and square excitations cases. Their shapes are all almost the same. In figures 7 and 8, we present respectively, for different periods of the applied heat flux, the average temperature and stress of compression at the quasi-steady state. We can observe the same behavior for the three heat fluxes for any values of the period.

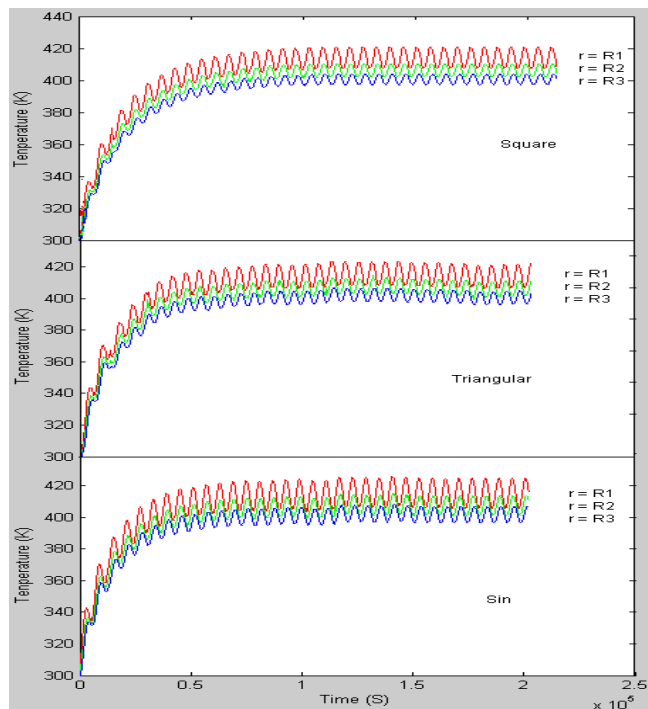


Figure 6: Evolution of the temperature under different forms of the heat flux ( $e_1=e_2=0.03$  m,  $\tau=60$  s).

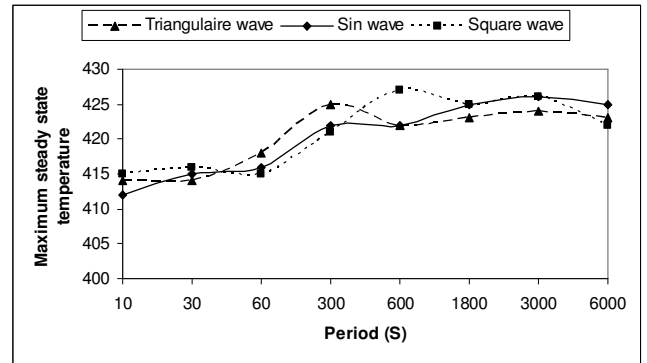


Figure 7: Variation of the maximum average temperature at steady state for  $z=L/2, r=R_1, e_1=e_2=0.03$  m

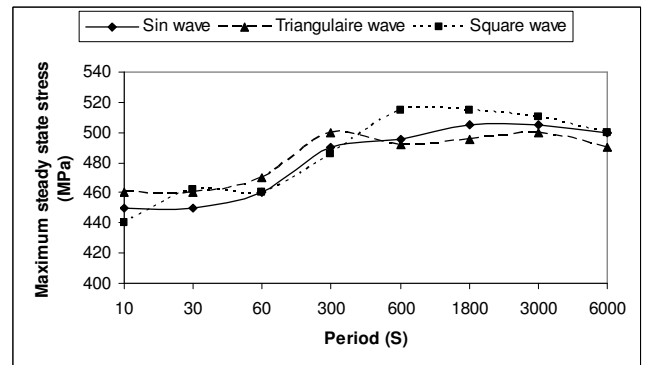


Figure 8: Variation of the maximum average stress at steady state for  $z=L/2, r=R_1, e_1=e_2=0.03$  m.

For these three shapes, figures 9, 10 and 11 show the damage obtained for a particular period  $\tau=6000$  s. For the other values of the period, the results are presented in figure 12 for the damage and in figure 13 for the lifetime of the multi-material. These curves have the same shape for the three cases of the analyzed heat fluxes.

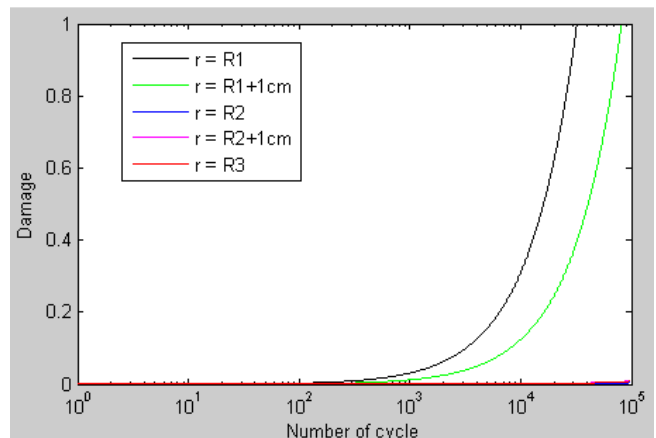


Figure 9: Evolution of damage at period  $\tau=6000$  s for the sinusoidal heat flux case,  $e_1=e_2=0.03$  m.

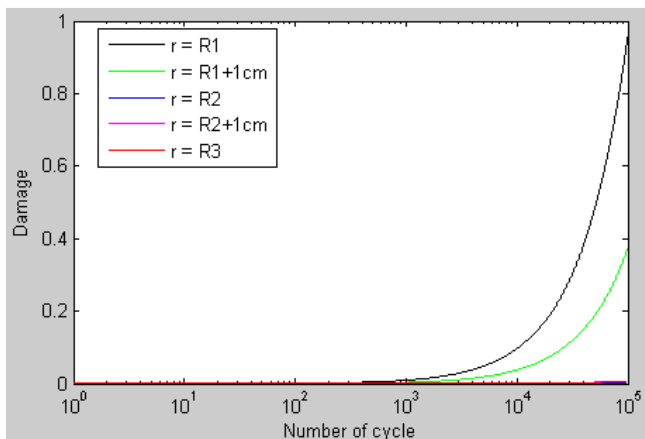


Figure 10: Evolution of the damage at period  $\tau=6000s$  for triangular wave heat flux, ( $e_1=e_2=0.03 m$ ).

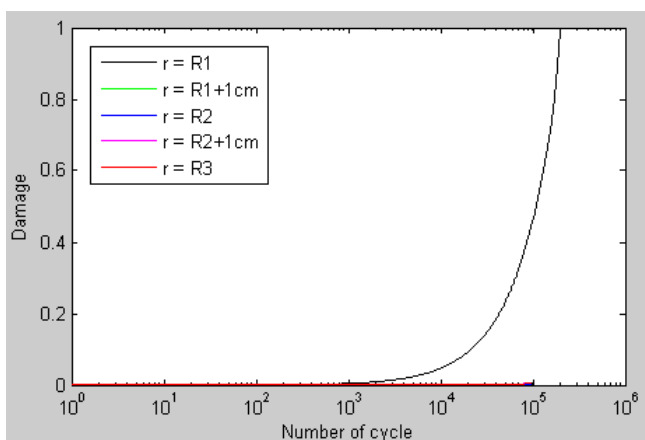


Figure 11: Evolution of the damage at period  $\tau=6000 s$  for square wave heat flux, ( $e_1=e_2=0.03 m$ ).

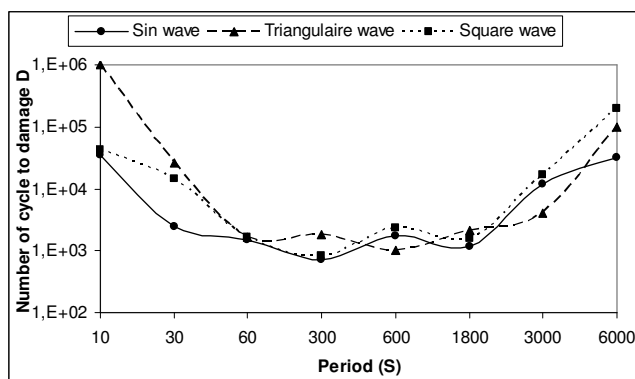


Figure 12: Variation of the number of cycles to obtain the damage in function of the period of heat fluxes,  $e_1=e_2=0.03 m$

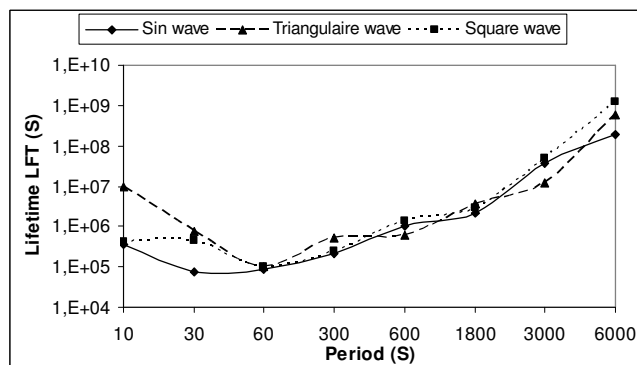


Figure 13: Variation of the time to obtain the damage (lifetime) function of the period heat fluxes,  $e_1=e_2=0.03 m$

### B- Influence of the period on the total thickness ( $e=e_1+e_2$ )

**of the multi-material:** The simulated computations, Figs 14 to 19, are obtained in the conditions described before and for the sinusoidal heat flux case. We can conclude the following remarks:

- While the total thickness of the body increases, the lifetime and the number of cycles to damage increases, Figs. 18 and 19. This effect can be explain by the fact that the maximum applied temperature and the stress at  $z=L/2$ , and  $r=R_1$  (critical point) decrease when the total thickness increases, Figs 16 and 17.

- Figs. 14 and 15 represent the amplitude of the temperature and the stress in the multi-material at  $r=R_1$  and  $r=R_3$ . We can conclude that, when the thickness increases, the amplitude of the temperature and the stress at  $r=R_1$  increases. As the total thickness of the multi-material increases, the influence of the convective heat transfer condition (cooling face  $r=R_3$ ) decreases and then the temperature and the stress amplitudes decrease as well.

Fig. 18 shows that the number of cycles to damage is a function of both the sollicitation period and the thickness. We can remark that when the period decreases, the number of cycles to damage increases starting from a certain value of the period (300 s), [21]. After this value, the number of cycles to damage becomes more and more stable with a slight increase accompanying the increase of the period. This is caused by the relaxation effect at high periods. The maximum amplitude of the temperature and the stress become also more stable when the period of the thermal load sollicitation reaches high values. This figure shows also that the domains of using a high number of cycles to damage can be obtained for the heat flux periods:  $\tau < 30$  and  $\tau > 2400$ .

Fig. 19 shows the lifetime of the material defined as the result of the multiplication between the numbers of cycles to damage, Fig. 18, and the period at each point:  $LFT = D \times \tau$ . For the small thicknesses ( $e=0.02 m$  and  $e=0.04 m$ ), the lifetime increases when the period increases, despite the increasing values of the temperature and the stress, Figs. 16 and 17.

For the lower periods (high frequency), the multi-material is operating under hard conditions, i.e. the multi-material is subjected to a faster damage corresponding to a weak lifetime,

although the temperature and the stress are relatively low, [14], [21].

For high thicknesses, ( $e=0.06\text{ m}$ ,  $e=0.08\text{ m}$  in Fig. 19), the lifetime is high in the domain of periods  $\tau < 30$  and  $\tau > 2400$ . In fact, for the lower periods, the temperature and the stress amplitudes of the oscillations, figs. 14 and 15, under thermal cycling heat flux, are weak and not sufficient to damage the multi-material, contrarily to the case of higher periods.

So, we can observe, for this geometry and for this thermal heat flux solicitation, a minimum value of lifetime corresponding to a particular period, for example  $\tau=30\text{ s}$  for  $e=0.08\text{ m}$  and  $\tau=60\text{ s}$  for  $e=0.06\text{ m}$ , Figs 13 and 19.

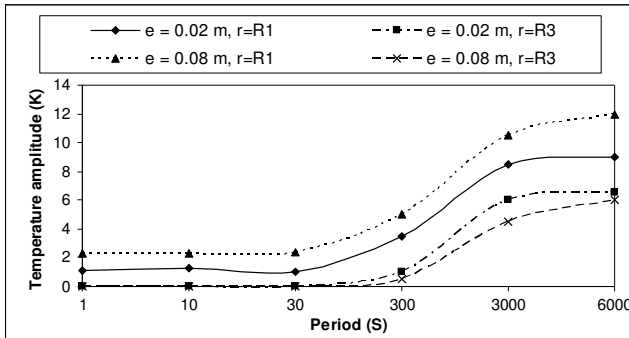


Figure 14: Variation of the maximum amplitude of the temperature at  $z=0.5L$ , for different periods of heat flux, ( $e_1=e_2$ ).

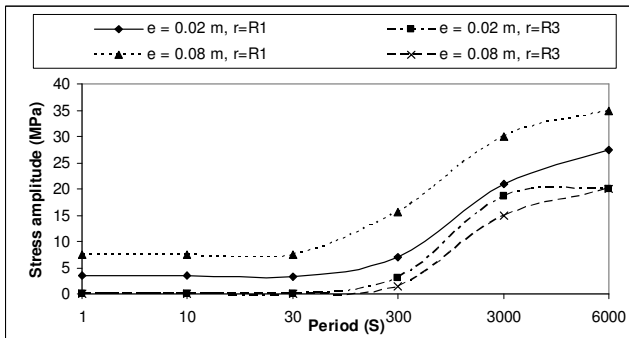


Figure 15: Variation of the maximum amplitude of the stress at  $z=0.5L$ , for different periods of heat flux, ( $e_1=e_2$ ).

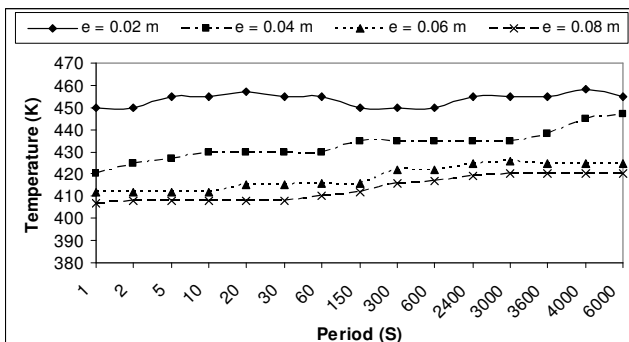


Figure 16: Variation of the average steady state temperature at  $z=0.5L$ , and  $r=R_1$ , for different periods of heat flux (sinusoidal case), and different thicknesses, ( $e_1=e_2$ ).

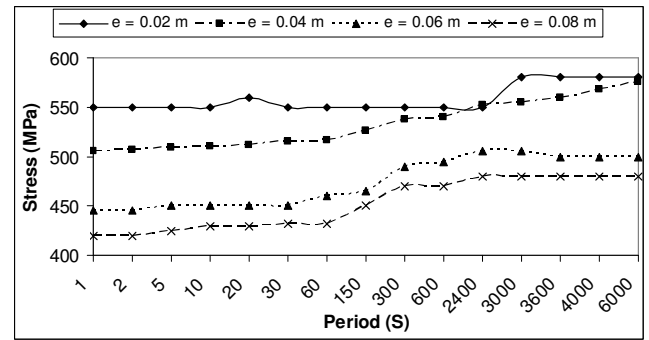


Figure 17: Variation of the average steady state stress at  $z=0.5L$ , and  $r=R_1$ , for different periods of heat flux (sinusoidal case), and different thicknesses, ( $e_1=e_2$ ).

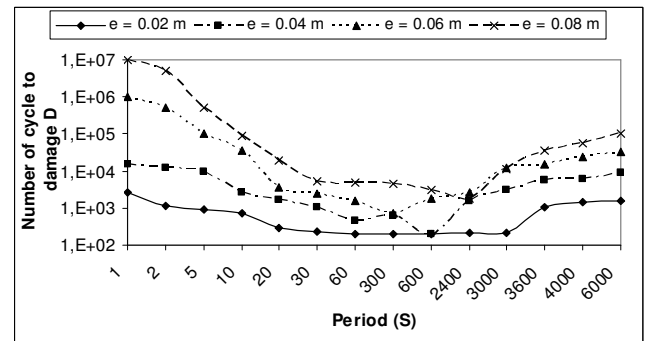


Figure 18: Variation of the number of cycles to damage in function of the period for sinusoidal heat flux and different thicknesses.

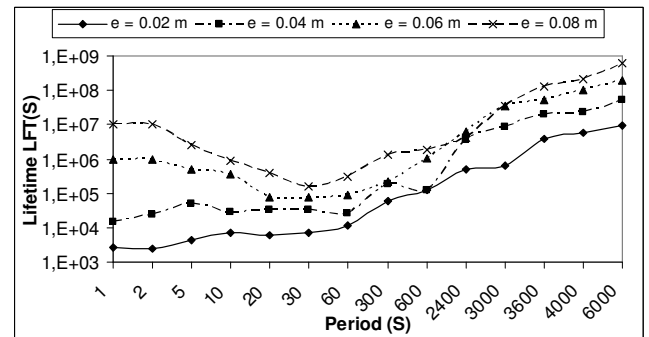


Figure 19: Variation of the lifetime function of the period for different thicknesses.

#### IV- CONCLUSION AND PERSPECTIVES

In this work, a numerical study of the damage of multi-materials in thermo-elasto-plastic regime is presented. The damage model is applied on the equivalent (or homogenization) material. The damage represented by the number of cycles and the lifetime; is presented for different shapes of the applied heat flux and for different thicknesses of the multi-material. The main results are summarized as follows:

- The numerical results show that the three shapes of the heat flux; sinusoidal, triangular and square, have the same results on the damage.

- The period of the thermal load has a remarkable influence on the damage. We demonstrate that around a range of periods, there is a hard influence on the lifetime of the

multi-material. This depends also on the geometrical properties of the studied material.

- Minimum values or range of periods for which the lifetime of the material is relatively low exist indeed.

As perspectives to this actual work, we are interested to study the effect of the amplitude of the heat flux and the effect of the convective heat transfer coefficient on the damage of the multi-material.

## REFERENCES

- [1] Dentsoras, A. J.; Kouvaritakis, E. P. (1995): Effects of vibration frequency on fatigue crack propagation of a polymer at resonance, Elsevier, Vol. 50, No. 4, pp. 467-473.
- [2] Primdahl, K.; Kustom, R. (1996): Cooling the APS Storage Ring Radio-Frequency Accelerating Cavities thermal stress/fatigue Analysis and Cavity Cooling Configuration, IEEE 0-7803-3053-6/9.
- [3] Singh, N.; Khelawan, R.; Mathur, G. N. (2001): Effect of stress ratio and frequency on fatigue crack growth rate of 2618 aluminium alloy silicon carbide metal matrix composite Defence Materials & Stores Research & Development Establishment, Indian Vol. 24, No. 2pp. 169-171.
- [4] Wang, R. J.; Shang, D. G.; Li, L. S.; Li, C. S. (2007): Fatigue damage model based on the natural frequency changes for spot-welded joints, Elsevier pp. 1047-1055.
- [5] Boulaajaj, A.; Cabrera, J.M.; Prado, J.M. (2007): Effect of initial microstructure, frequency and temperature on the low cycle fatigue behaviour of the soldering alloys 96.5Sn-3.5Ag and 63Sn-37Pb, Elsevier pp. 220-228.
- [6] Lemaitre, J.; Chaboche, J.L. (1988): Mécanique des matériaux solides, DUNOD, deuxième édition, BORDAS, Paris.
- [7] Saanouni K.; Chaboche, J.L. (2003): Computational damage mechanics. Application to metal forming. Numerical and Computational methods. Elsevier, vol. 3, n. 7, p. 321-376 Oxford.
- [8] Vidal, E. (1996): Prévion de la durée de vie en fatigue multiaxiale sous sollicitations d'amplitude variable à l'aide d'un critère global. Doctorat Thesis, INSA de Lyon.
- [9] Jabbado, M. (2006): Fatigue polycyclique des structures métalliques: durée de vie sous chargement variables, Doctorat Thesis, Ecole Polytechnique.
- [10] Jaskea, C.E.; Deevib, S.C.; Shadema, S.S. (1998): Fatigue and cyclic deformation behavior of iron aluminide, <sup>a</sup>CC Technologies, Dublin, OH 43016-8761, USA, <sup>b</sup>Research, Development and Engineering Center, Philip Morris USA, Richmond, VA 23234.
- [11] Charkaluk, E.; Bignonnet, A.; Thomas, J. (2004): Dimensionnement à la fatigue thermomécanique de structures dans l'industrie automobile, J. Mécanique & Industries, 5, 27-40.
- [12] Abboudi, S.; Bonnet, P. (1996): Approche locale de l'endommagement sous des conditions thermiques variables, C.R. 10èmes Journ. Nat. Comp. (JNC10), pp 597-605.
- [13] Abboudi, S.; Bonnet P. (1997): Transient Thermomechanical Homogenization of Multilayer Material. Second International Symposium on Thermal Stresses and Related Topics, Rochester, pp. 455-458.
- [14] Sheffler, K. D.; Alexander, J. A. (1972): Vacuum thermal-mechanical fatigue testing of low iron base high temperature alloys, topical report no.3 for national aeronautics and space administration, Nasa, under contract nas-3-6010.
- [15] Taher, B.; Youness, R.; Abboudi, S. (2006): Numerical analysis of thermomechanical behavior of a multimaterial under thermal cycling conditions, PVP2006 – ICPVT – 11, ASME Pressure Vessels and Piping Division Conference, Vancouver, Canada, ASME digital store PVP2006-ICPVT-11-93495, 10p., in CD-ROM.
- [16] Taher, B.; Abboudi, S.; Younes, R. (2007): Study of homogenization technique in a tow-layer cylindrical material, IMECE 2007, International Mechanical Engineering Congress and Exposition, ASME digital store IMECE2007-44084, Seattle, Washington, USA, 10p., in CD-ROM.
- [17] Hetnarski Richard B. (1986): Thermal stresses I, Elsevier, Rochester institute of technology, New York, USA.
- [18] Hetnarski Richard B. (1999): Thermal stresses IV, Lastran, Rochester institute of technology, New York, USA.
- [19] Hetnarski Richard B. (1999): Thermal stresses V, Lastran, Rochester institute of technology, New York, USA.
- [20] Bonnet, P. (1998): Contribution à l'étude des couplages thermiques et mécaniques dans les multimatériaux sous sollicitations thermiques variables, Doctorat Thesis, Université of Technology of Belfort-Montbéliard, UTBM.
- [21] Kawasaki, N.; Kobayashi, S.; Hasebe, S. (2006): Spectra Thermal Fatigue Tests under Frequency Controlled Fluid Temperature Variation -Transient Temperature Measurement Tests, Proceedings of 2006 ASME Pressure Vessels and Piping Division Conference (PVP2006) Vancouver, Canada, ICPV11-93548, 8p., in CD-ROM.
- [22] Gaddis E. S.; Brian Spalding D.; Taborek J. (1989): Heat exchanger design handbook Physical properties tome 5.